Co-simulation of Electrical propulsion and power systems in Direct Drive applications

Pablo F. Miaja
Power supply systems group
University of Oviedo
Gijón, Spain
fernandezmiapablo@uniovi.es

Andreas Franke
Electrical Power Management section (TEC-EPM)
European Space Agency
Noordwijk, The Netherlands

Denis Estublier
Electric Propulsion section (TEC-MPE)
European Space Agency
Noordwijk, The Netherlands

Christian Brandt
Electrical Power Generators section (TEC-EPG)
European Space Agency
Noordwijk, The Netherlands

Jorge Ruiz Torralba
Empresarios Agrupados Internacional
Madrid, Spain

Maria Aranda Rosales
Empresarios Agrupados Internacional
Madrid, Spain

Manuel Arias
Power supply systems group
University of Oviedo
Gijón, Spain

Abstract: **Electric propulsion has gained a lot of traction in spacecrafts. Among them, Hall Effect Thrusters (HETs) are widely used. Its operation involves several engineering domains including fluid and thermal dynamics and electrical engineering, not to mention the complicated physics of the discharge process. Moreover, Electrical Propulsion power needs make it a driver in the design of the spacecraft power system.**

Therefore, co-simulation of the electrical propulsion system alongside the electrical power system, including power generation, opens the door for system optimization and unveils interactions between the electrical power and propulsion systems. This is specially the case for the so-called Direct Drive (DD) architectures, in which the power from a solar array is directly fed to the HET without or with little power conversion stages.

This paper presents an ECOSIM made model joining together ESA-PEPS libraires for Electrical power system and a subset of ESPSS propulsion libraries (ESA_EP_PIE). The models are used to size the power system for a given mission and to evaluate the interaction of Maximum Power Point Tracking methods with Direct Drive architectures.

I. INTRODUCTION:

The objective of the paper is to present ECOSIM models that can be used to simulate electrical propulsion and electrical power systems at the same time. It builds on pre-existing libraries used for Electrical propulsion (ESA_EP_PIE), provided by Empresarios Agrupados Internacional, and for power system simulation (ESA-PEPS), provided by ESA TEC-EPM. The first one includes HET models, gas tanks, fluid lines, etc. It allows for simulating propulsion related figures such as thrust and specific impulse. ESA-PEPS deals with simulation of Solar Arrays (SAs), batteries, power converters, loads and includes orbital simulations for determining the solar flux incident on the SAs.

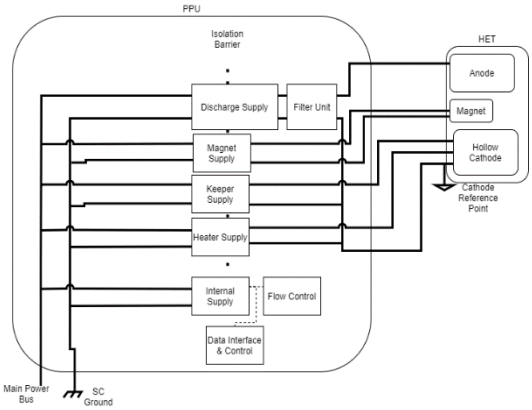

Figure 1: Typical PPU

A typical PPU schematic is represented in Figure 1. The PPU is in charge of controlling the HET to achieve the desired thrust. It controls the gas flow both for the thruster and the hollow cathode

interacting with the gas supply system. It provides the current to the magnet via the Magnet Supply to achieve the desired magnetic field in the HET. It prepares the plasma ignition through the heater, provided by the Heater supply, and powers the electron generation in the hollow cathode though the Keeper Supply. Finally, it provides the anode with the voltage and current necessary to generate and maintain the discharge between Anode and Cathode, which in turn generate the thrust. The power consumed in this discharge is supplied through the Discharge supply.

The Discharge Supply is the element that processes most of the power, HETs range from hundreds of watts to few kW, being 5 kW a common power. Therefore, its efficiency is critical towards the spacecraft (SC) design. The high power processed impacts the thermal design of the PPU and the total SC. The physics of the discharge between Anode and Cathode is very complex [1], [2]. This discharge will have an IV curve that above a certain voltage, behaves like a current source, demanding a DC value proportional to the gas flow. This voltage is usually in the range of hundreds of volts, being 300 V a typical value. In addition, several oscillations will appear. The most important have frequencies mostly in the tens of Kilohertz range and have an amplitude up to 100% of the DC current value. The mission of the Filter Unit is to avoid these oscillations to propagate into the discharge supply. Therefore, the Discharge supply will see the discharge between anode and cathode almost as a pure DC current source. To guarantee the discharge between anode and cathode and prevent a discharge between the anode and the structure, the discharge supply output will be referenced to the Cathode Reference Point (CRP) instead of the SC ground, therefore the discharge supply typically is a galvanically isolated one.

In traditional architectures, the discharge power is converted from the Solar Array (SA) or the battery first by the Power Conversion and Distribution Unit (PCDU) and then by the Discharge Power supply. Thus, there are two cascaded power conversions with the associated efficiency penalty and the power demand of the discharge supply affects the PCDU design and the whole SC design. Therefore, DD topologies have been proposed to supply the discharge power demand directly from a dedicated SA [3], [4], so there are no power conversions between the SA and the discharge, thus avoiding the design of the Discharge Supply and preventing this power by being processed by the PCDU. One of the main disadvantages of this system is that the SA that must supply the EP has to provide

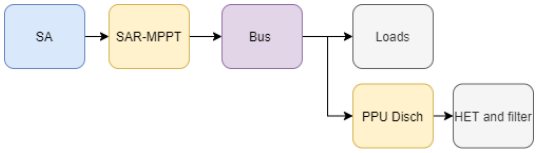

Figure 2: Traditional PPU architecture

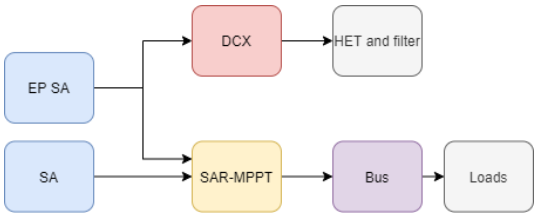

Figure 3: MPPT separated LV SA

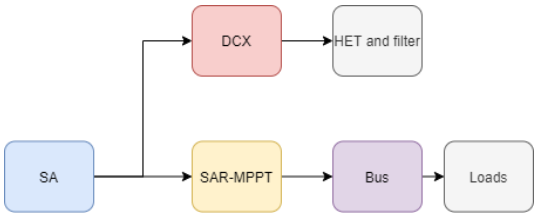

Figure 4: MPPT single LV SA

voltages above 300 V, which is a technological challenge in the space environment [5], [6].

Hall Effect Thrusters (HET) are chosen as a baseline for this study since they operate at a lower voltage (around 300 V) than other EP alternatives such as the Gridded Ion Thrusters. Then, the voltage gap between what can be achieved by state of the art and envisioned development of SAs and the operating voltage of the HET is rather small. However, for this work 100-V SAs are selected, representing the current mature technology. In between the SA and the HET an unregulated DC/DC converter (DCX) will scale the SA voltage to the HET needs. Moreover, it will also provide galvanic isolation, guaranteeing the discharge between Anode and Cathode. Moreover, galvanic isolation includes a degree of protection thus avoiding short-circuiting the SA.

In this work several DD alternatives have been simulated in ECOSIM at system level. Two objectives were sought: investigate interaction between MPPT techniques, explained in section V, and perform orbital simulations to size the power system as explained in section VI, where a small comparison among the architectures explained in section II are shown. A brief description of the most important developed models is carried out in section III.

II. Overview of the Topologies:

An overview of the different topologies under study is performed in this section. The block schemes in Figure 2, Figure 3 and Figure 4

represent with arrows the most application relevant power flows between the different constituents of the spacecraft. Low voltage SAs, with MPP close to 100 V are depicted in blue. Solar Array Regulators (SARs) are represented in yellow. These SARs take an input unregulated voltage and deliver it at the output tightly regulated. Unregulated voltage transformations stages, DCX, are represented in red. As aforementioned DCX provide at its output a scaled version of the voltage at its input. The bus, represented in purple, performs the distribution of electrical power to the loads which consume the electrical power. The loads are represented in grey. A detailed description of the architectures and the selection criteria is carried out in [7].

The traditional architecture is shown in Figure 2. In the traditional architecture the PPU Discharge supply provides the HET with a regulated voltage extracting power from the bus. This model is introduced for comparison purposes. Architectures based on solar array regulators with DC/DC converters with MPPT capabilities are shown in Figure 3 and Figure 4.

Two systems based on SAR MPPTs and the connection of the HET to the SA through a DCX are used in this work to showcase different considerations. In the Single LV SA architecture depicted in Figure 4 a low voltage SA is scaled up to supply a HET, at the same time the remainder of the power is used to supply the bus. The same approach is used in the Separated LV SA architecture shown in Figure 3. In this case the SAR-MPPT has two independent inputs, and the EP SA is sized to supply the HET power demand. The SAR-MPPT will supply the bus by demanding all the unused power from the EP-SA and matching the bus demand with the power extracted from the SA.

III. New components Developed:

1) PPU_HET_SINK:

The main developed component is the model for the PPU, called PPU_HET_PSINK and represented with internal constituents, which can be seen in Figure 5. It is derived from the PPU of the ESA-PIE library. However, there are two main differences. First, the discharge supply has an input that connects the output for the discharge supply port, th_anode, to a specific input situated between disch_in_pos and disch_in_neg electrical ports. The current that flows out through th_anode circulates in from disch_in_pos and out from disch_in_neg. The voltage of th_anode is the voltage between disch_in_pos and disch_in_neg. This is achieved through a CellAdapter model from PEPS. Thus, the power demand between these two ports, will be the discharge power. This allows to connect the discharge supply to whatever source available, being a SA or the voltage bus, so the different power architectures can be evaluated in ECOSIM. The second main difference is the input created by the electrical ports bus_demand_pos and bus_demand_neg. The aggregated power demand for all the supplies inside the PPU, namely heater ignition keeper, magnet, heater valves and throttle. All these sources are aggregated in a PEPS power load to be connected to the bus or other supply. Finally, logic ports for turning on and off the gas flow through the valves model and the reference for the throttle control are included.

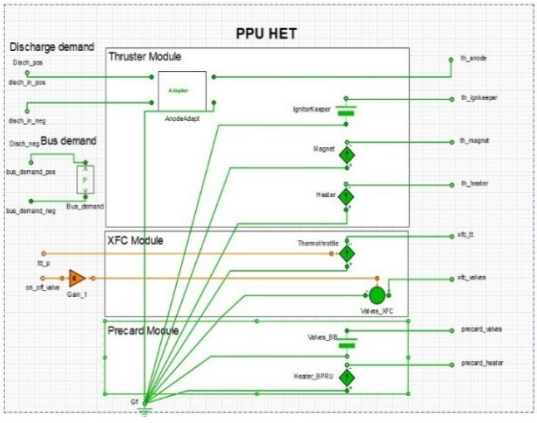

Figure 5: PPU_HET_PSINK implementation

2) EP_THRUSTER_single:

The EP thruster model, represented in Figure 6, is just a modification of the one included in the ESA-PIE library. The ports have been individually addressed so it can be connected individually to the PPU. The thruster can be turned on and off through the gas flow. In any case as the original model the voltage and the gas flow have to be at a certain level for a specified time so the HET ignites.

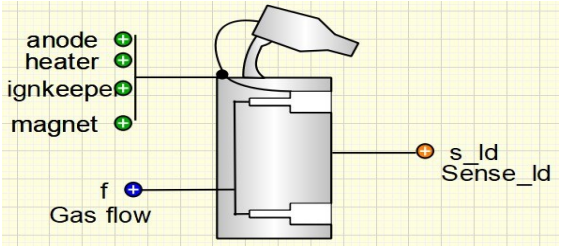

Figure 6:EP_thuster_single

3) DCX:

The DCX model, represented in Figure 7, has been developed. It mimics the behaviour of the DCX, so the voltage between e_p2 and e_n2, port 2, is a scaled version of e_p1 and e_n1, port 1. As

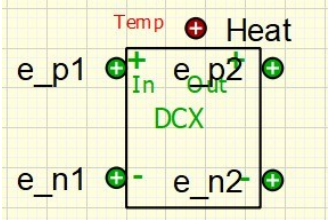

Figure 7: DCX model

an oversimplification, the efficiency of the DCX is constant regardless of the power processed. The power demand at port 1 is the power demand at port 2 plus the losses. It is a derivation of the DCDC model from the PEPS library.

4) MPPT3:

To simulate the architectures in which different SA sections interface to the power bus with a SAR with independent MPPT capabilities the MPPT3 model, represented in Figure 8, was developed. This model is based on the MPPT model of the PEPS library. It has input ports for getting the characteristics of two different SA. Three electrical ports are defined. Port 1 is defined with e_p1 and e_n1, Port 2 between e_p2 and e_n2 and port 3 between e_p3 and e_n3. The power flow only can happen in the following way: The power absorbed by ports 1 and 3 will be delivered to port 2. A control loop will regulate the voltage at port2 to a predefined one (taper voltage). The control loop voltage will determine the voltage at ports 1 and 3, limiting it to the maximum power point voltage of each SA. Power will be preferably extracted from port 3. In case port 3 locks into MPP the system will start drawing power from port 1 to supply the demand in port 2.

IV. Power System Simulations

The ESA-PIE model taken as a reference can only produce a discharge current of 3.5 A. This limit has not been surpassed. The current can be controlled by the gas flow and in these simulations is regulated to 2.5 A. The example of the EP system included in the ESA-PIE library is the same used for the EP system. The only modifications are the replacement of the XFC and HET models for the ones presented in this work and the replacement of the PPU by the *PPU_HET_SINK* model developed for this task. As previously mentioned, this model offers different electrical ports, one for the discharge supply and the other for aggregating the power demand of all the sources internal to the PPU.

The rest of the power system is the same in all cases. The battery is simulated by a 1000 nF capacitor with an EOC voltage of 100 V. In all cases the battery initial voltage is 99.9 V. The SAs are based in AzurSpace 3G30 solar cells. The thermal model does not include thermal nodes and the temperature is fixed to 25ºC..

V. MPPT Interactions:

Most of the SC power systems using MPP converters track the MPP using a similar method to the incremental transconductance detailed in [8]. This method is described in [9] and reproduced in Figure 9. This method produces oscillations around the MPP voltage. If a HET is

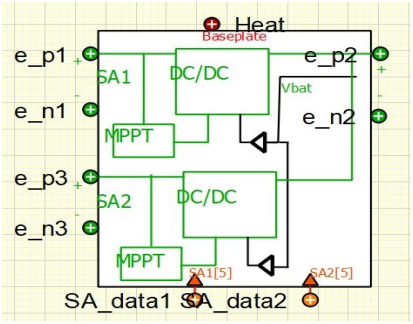

Figure 8: MPPT3 model

connected, through the filter unit, to a SA and the MMPT system is inducing these oscillations the HET will be seeing them. The discharge voltage will not be constant, it will include these oscillations. Moreover, if the HET is connected to the SA through a DCX the oscillations will be scaled through its turn ratio.

The amplitude and frequency of these oscillations vary from system to system. The described MPPT system acts in conjunction with the current control loop of the converter, being $V_{control}$ in the reference to the loop. Therefore, the evolution of $V_{control}$ must have a bandwidth much lower than the control bandwidth, so frequencies in the low kHz or hundreds of Hz are common. In [9] oscillations of 8 V, around a MPP of 120 V, and a frequency of 183 Hz are reported. If a 1:3 DCX is used these 8 V will translate into 24 V.

In order to assess how these oscillations will affect the HET performance an EP system provided by Empresarios Agrupados has been used in ECOSIM. The complete model is shown in Figure Figure 1 The PPU voltage is provided by an AC voltage source with a DC offset of 300 V and an amplitude of 60 V. The filter unit has a cut-off frequency of 726 Hz and it is designed to damp the discharge current oscillations. These discharge current oscillations have not been modelled in ECOSIM.

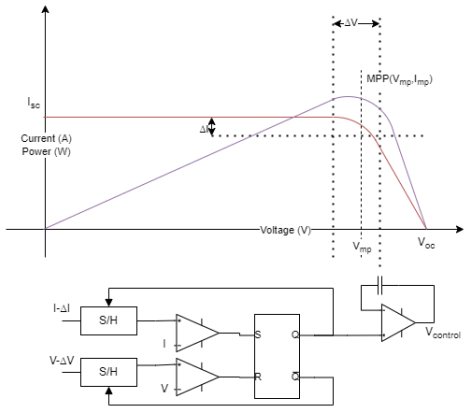

Figure 9: Most common MPPT system.

The voltage anode supply voltage in the PPU (red) and the voltage in at the HET anode (blue) are shown in Figure 11. It can be seen how there are substantial oscillations despite the action of the filter unit. The discharge current, represented in Figure 12 shows a constant current source as expected. The voltage variation translates into the specific impulse (blue) and thrust (red) of the HET, as it can be seen in Figure 13 which includes with a close up. As expected, it oscillates following the discharge voltage. Whether this behaviour is detrimental towards the EP system is outside the scope of this work and must be assessed by EP experts.

By having a Filter Unit with a lower cut-off frequency than the lower expected oscillations will help to solve the problem. The same simulation was repeated having a cut-off frequency of 72.6 Hz and its results can be seen in Figure 14 where it can be seen how the filter attenuates the oscillations at the output of the PPU, so they do not reach the anode of the HET. Whilst the current remains the same, thanks to the lower voltage variation both the thrust and specific impulse show less variations as seen in Figure 15.

The effects in the mass of having a bigger filter unit are out of the scope of this work. If some of the MPPT topologies are chosen EP experts need to determine if the HET could operate with the MPPT oscillations and what would be the impact on its performance.

VI. Orbital Simulations

To verify the advantages of the different approaches in a realistic environment a mission was built using PEPS, ESA-PIE and the previously introduced models explained in section III.

The mission is similar to GOCE [10], [11], a SC flying at a 90 degree inclination in a circular orbit of 250 km an a LTAN of 6:00:00. So almost a Dawn-Dusk Sun Synchronous orbit. Reference and epoch dates are set at 1 of January 2000 at 12:00:00. So, the SC will face eclipses each orbit. Orbital period is 5370 s and eclipses last approximately for 1293 s. The SA will be a fixed

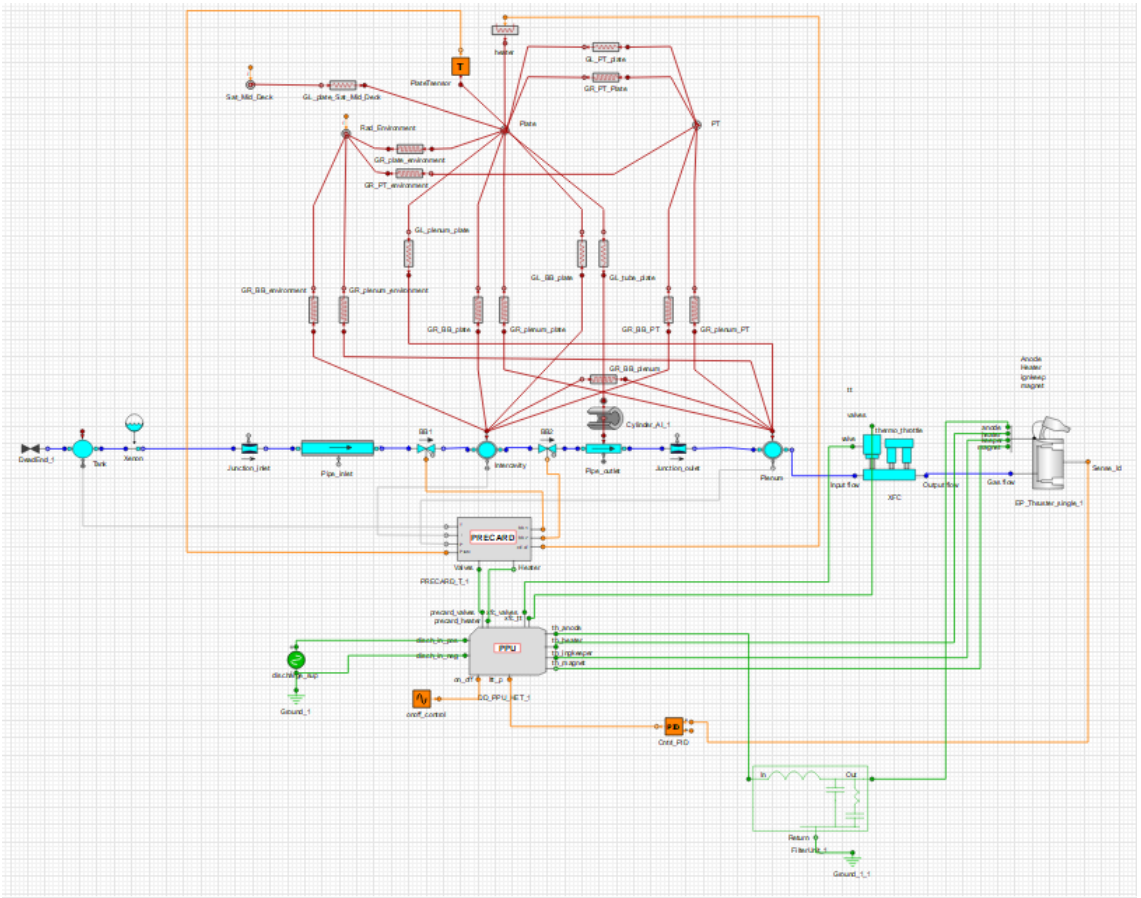

Figure 10: ECOSIM model of the EP system for testing MPP oscillations

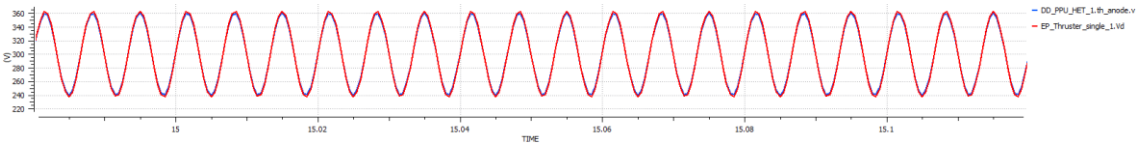

Figure 11: Anode voltage

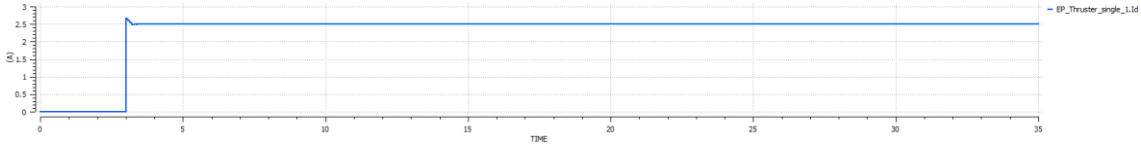

Figure 12: Discharge current

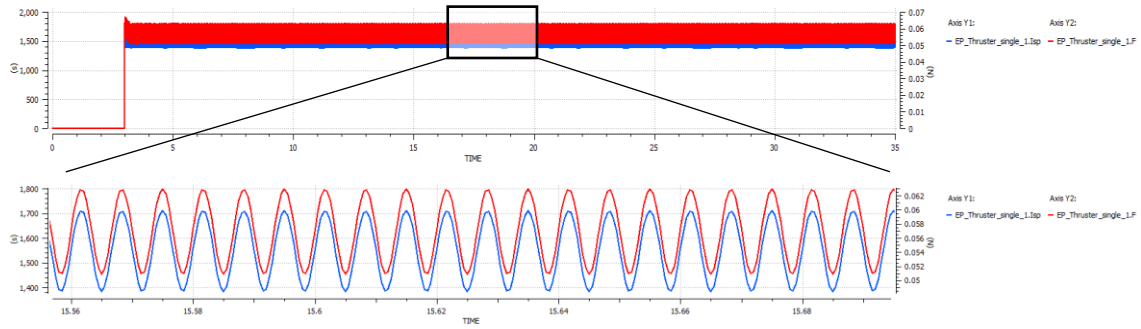

Figure 13:Thurst and specific impulse

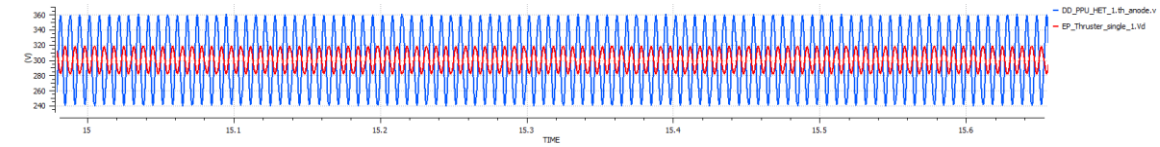

Figure 14: Anode voltage at lower FC

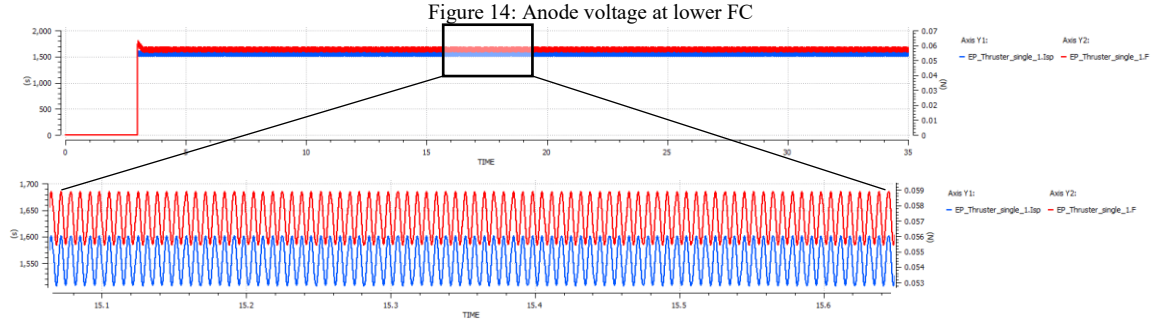

Figure 15: Thrust and specific impluse at lower FC

body one, with its normal direction will point normal to the orbital plane. The Solar Aspect Angle varies very little around 23 deg. Such a low orbit claim for almost constant thrusting to compensate atmospheric drag, as GOCE did.

At all times the SC will be consuming 800 W. The power system will be a MPPT based battery bus regulated at 100 V. The battery is simulated by a 1000 F capacitor to avoid using the battery cell models of PEPs that include proprietary information. In these simulations oscillations around MPP are not considered.

The PPU model bus port is connected to the output port of the SAR, which is the main power bus. This means that when the EP is on, the additional power demand of the EP system (magnet, valves, control,…) will come from the power bus. The discharge input port will be connected to different power sources to configure the different architectures.

EP propulsion shall be on only during sunlight. Discharge current is regulated to 2.5 A via the gas flow control. Voltage to the discharge will only be regulated in the traditional PPU architecture and in the PPU-DCX architecture to 300 V. So, the discharge power is 750 W at 300 V. As before the ESA-PIE EP model does not allow for more than 3.5 A.

The same SC was analysed using 2 different architectures. The first is the traditional PPU, represented in block form in Figure 2 and in ECOSIM in Figure 16. The discharge supply is modelled using a DCDC model with an output voltage of 300 V. The input of the DCDC converter is connected to the bus and the output to the input discharge port of the PPU. Then all

the power will come from the bus. This architecture is what is in use today and will serve as a reference against two of the proposed ones. Other architecture is the Single_SA_LV represented in Figure 17, which in block form corresponds to Figure 4. In this case a DCX connects the output of the SA to the input of the discharge input of the PPU. It has again a ratio of 3 so for the 110 V as the V_{mp} of the SA it will produce 330 V in the thruster. The remaining power of the SA will be transferred to the bus. The last architecture is the Separated SA Low Voltage represented in and Figure 3 in Figure 18. In it two 110 V V_{mp} SA interface through separate SAR modules with individual MPPT capabilities to the power bus.

Solar Arrays are simulated using the ones in PEPS library with 1 thermal node. Solar Cells are AzurSpace 3G30. No irradiation degradation no strings lost are considered. To obtain the desired voltage strings of 56 cells are used.

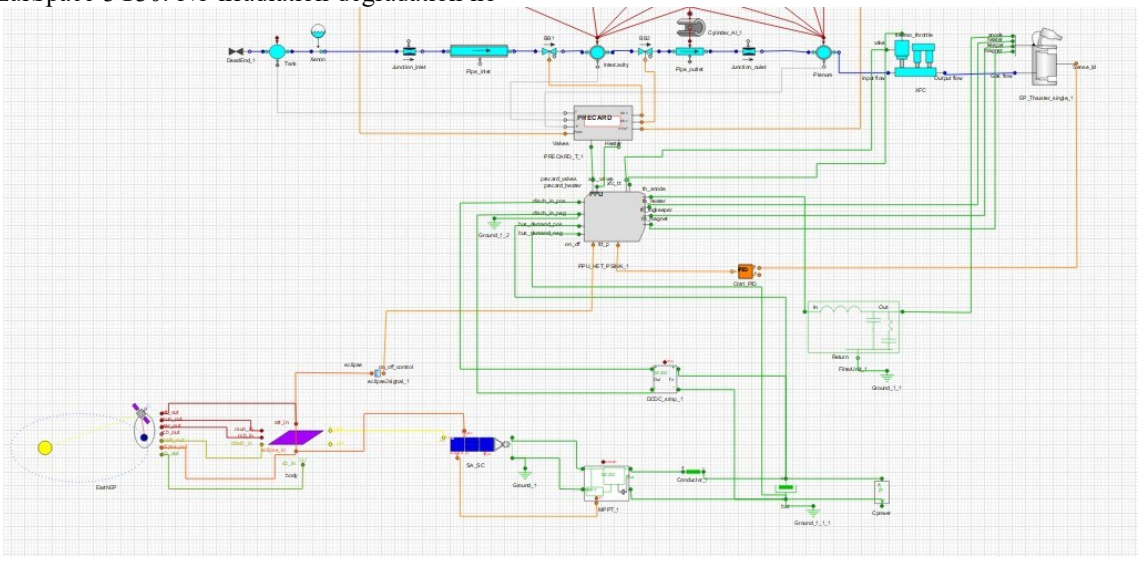

Figure 16: Traditional PPU architecture

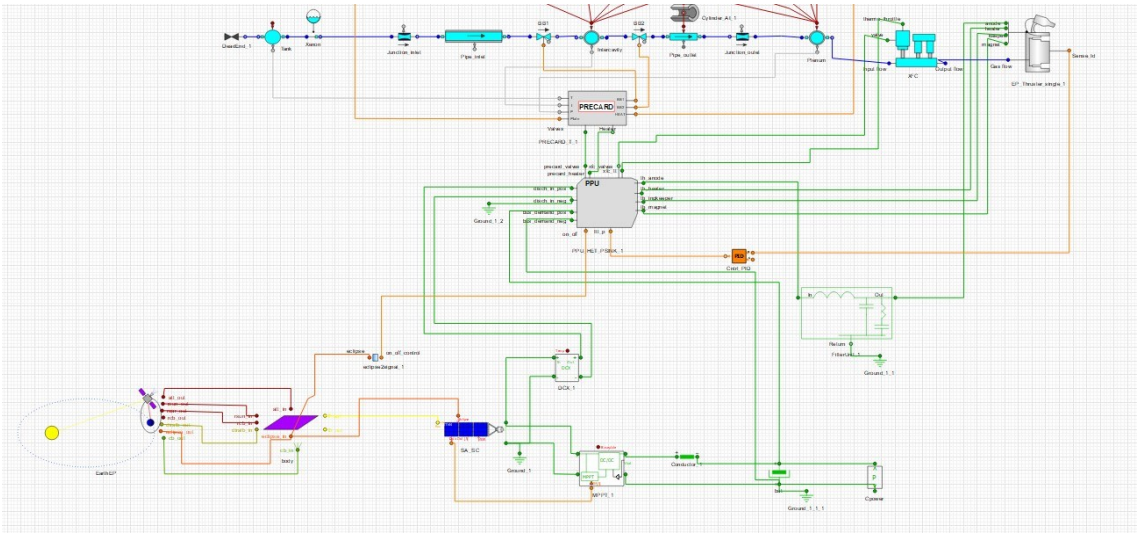

Figure 17: Single SA architecture

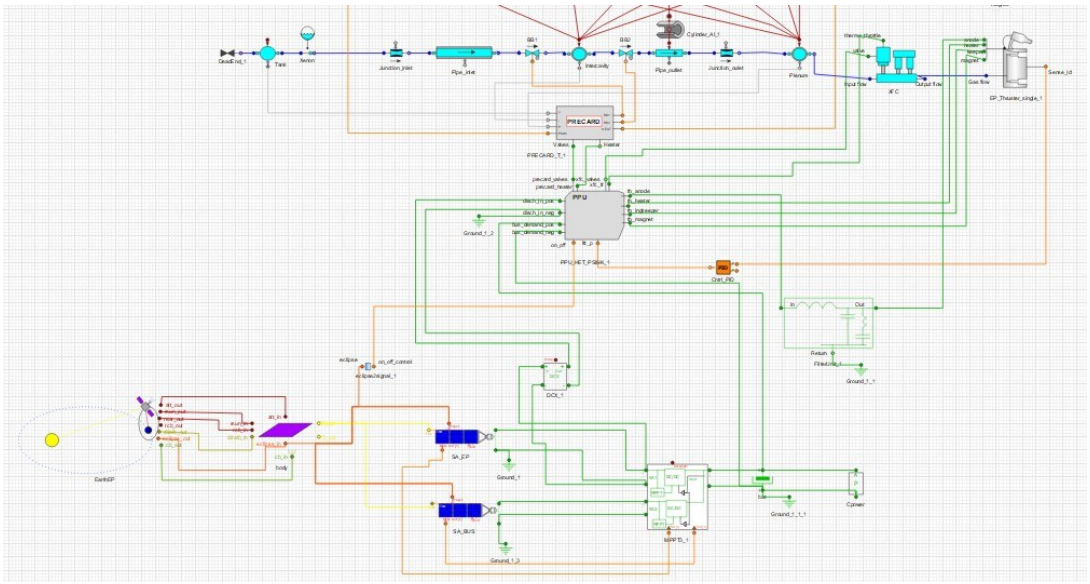

Figure 18: Separated SA architecture

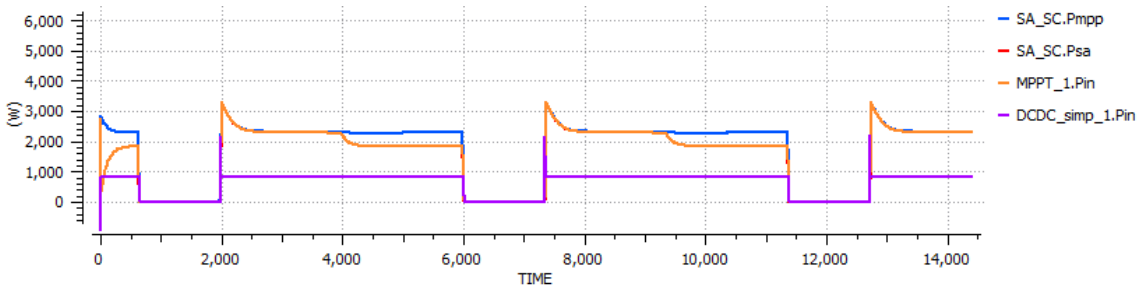

Figure 19: Powers in traditional PPU architecture

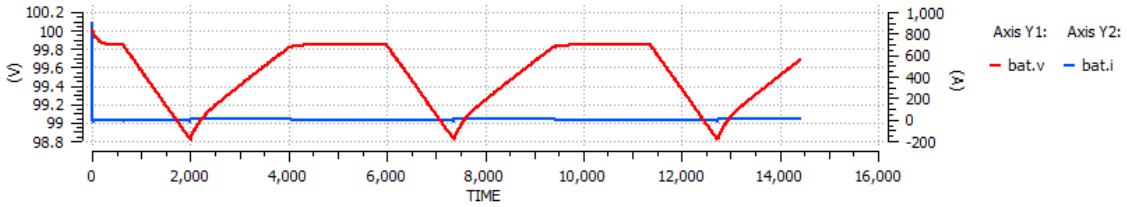

Figure 20: Battery voltage and current Traditional PPU

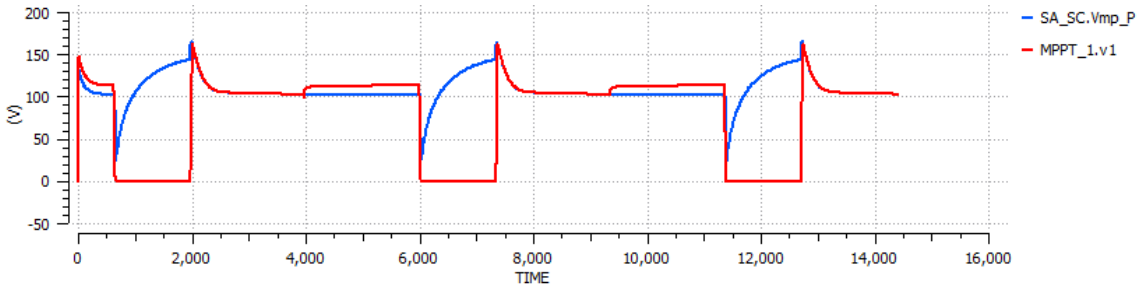

Figure 21: Voltage over SA in traditional architecture

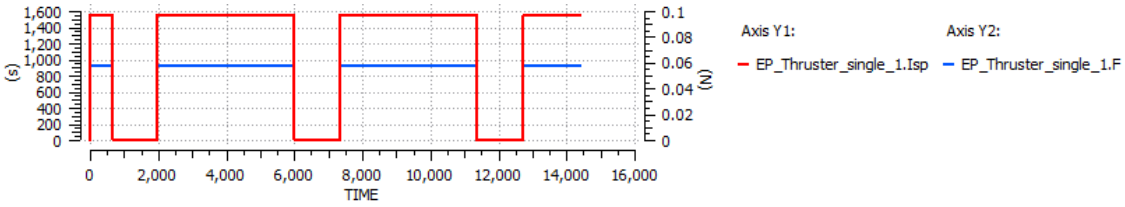

Figure 22: Thrust and ISP in the Traditional architecture.

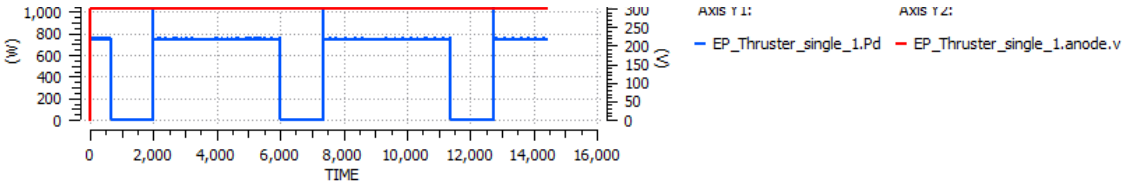

Figure 23: Discharge power and anode voltage in the Traditional architecture

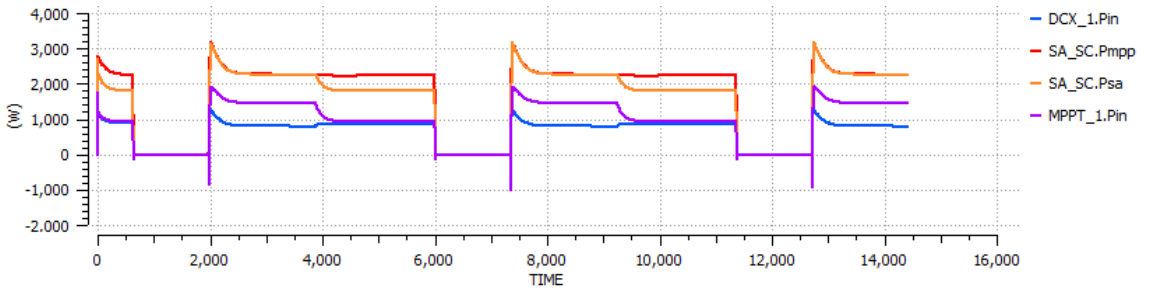

Figure 24: Powers in Single SA architecture

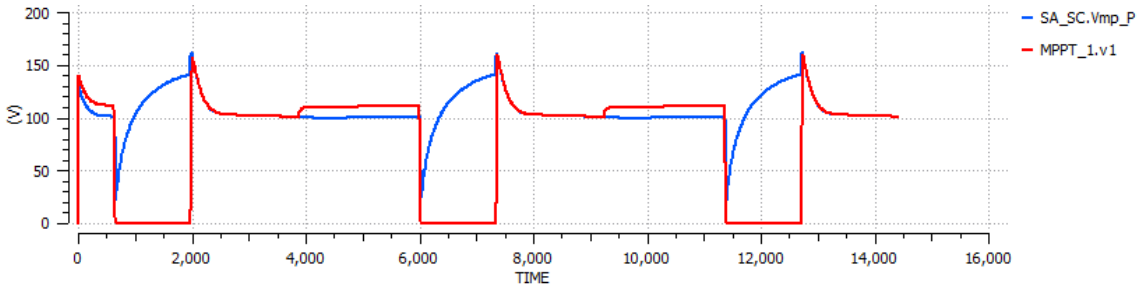

Figure 25: Voltage over SA in Single SA architecture

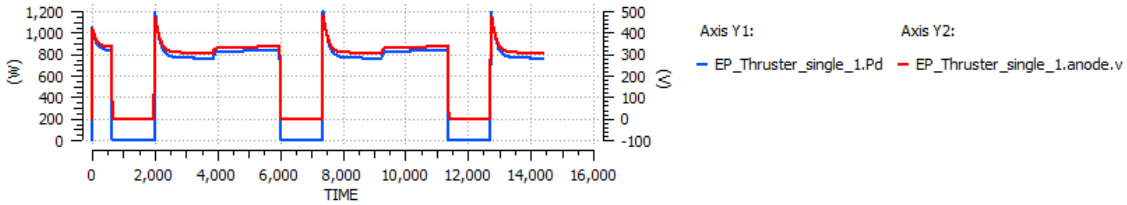

Figure 26: Discharge power and anode voltage in the Single SA architecture

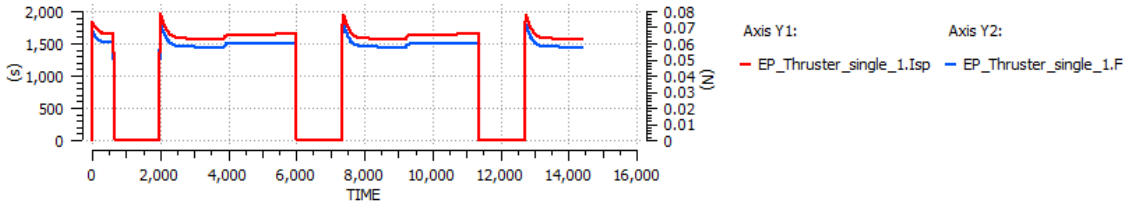

Figure 27: Thrust and ISP in the Single SA architecture

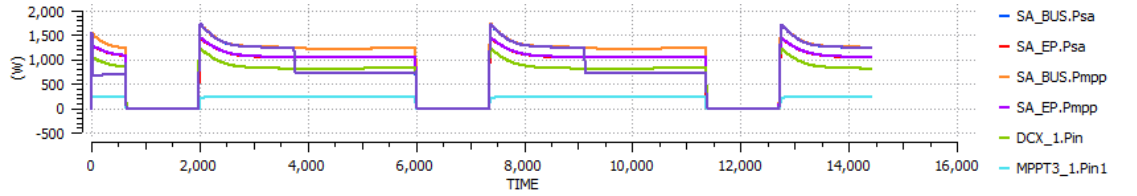

Figure 28: Powers in Separated SA architecture

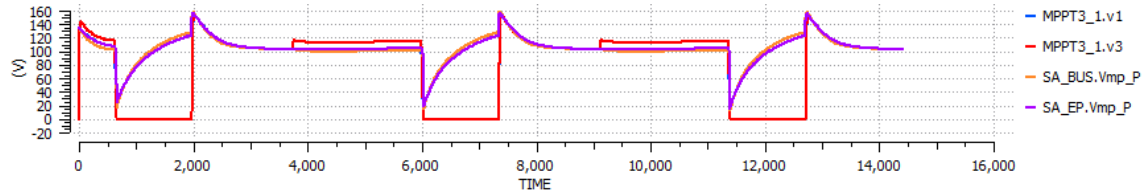

Figure 29: Voltage over SAs in Separated SA architecture

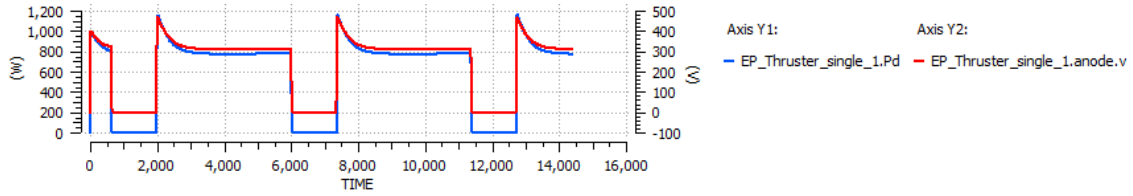

Figure 30: Discharge power and anode voltage in the Separated SA architecture

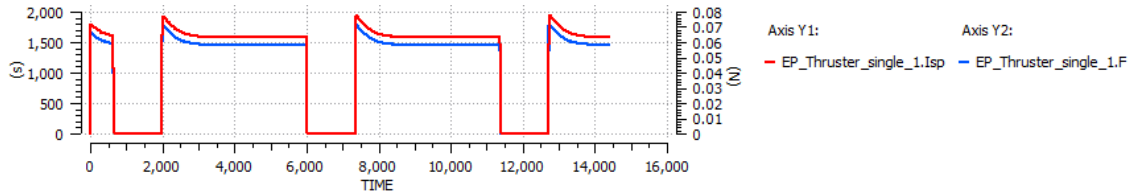

Figure 31: Thrust and ISP in Separated SA architecture.

Results with the Traditional PPU can be seen in the several figures. Figure 20 shows the typical behaviour of the battery voltage. While in eclipse the battery supplies the power to the loads and discharges itself. Once in sunlight the SAR locks into MPP and deliver power to the loads, which in this case includes the discharge of the EP. Once the battery is charged to its EOC voltage (100 V in this case) the current drops to 0. The power provided by the SAs is shown in Figure 19 along with its MPP. It can be seen how right after eclipse the maximum power is extracted from the SA, while the MPP diminishes when the SA gets hotter. This power goes into the bus through the SAR; the yellow trace represents the SAR input power. The EP discharge is supplied from the bus, the purple trace shows the power demand by the discharge supply. It can be seen that is constant, there is only the ignition current peak.

The voltage over the SA and its V_{mp} is represented in Figure 21. It can be seen how once the battery is charged, the SA voltage increases to reflect the descend in current demand following its IV curve.

Finally, the voltage and power demand for the discharge of the thruster is represented in Figure 23. It can be seen how the voltage is totally constant and once the thruster is ignited the power is constant too. This reflects in constant values for the thrust and the ISP represented in Figure 22.

With the other architectures there is a big difference on how the thruster is managed. In the traditional PPU architecture the voltage anode is regulated by the discharge supply. The current is regulated via the gas flow control. Then the power to the discharge is regulated. However, in the Single SA and Sep SA the voltage to the EP is proportional to the SA voltage. As the SC leaves out eclipse the SA is cold, its V_{mp} goes higher and the SA is capable to supply more power to the EP. As there is no voltage regulation the anode will see a higher voltage.

Figure 24 represents the power extracted from the SA (yellow), the power at the input of the DCX, so the EP discharge power (blue) and the power at the input of the MPPT SAR delivering power to the bus (purple). For comparison purposes the peak power point of the SA is represented in red. It can be seen how right out of eclipse the SAR locks the MPP of the SA. At the beginning, as the SA is cold (Figure 24) there is a peak. It can be seen how the total demand goes partly to the bus to charge the battery and supply the load and partly to the EP through the DCX.

Once the battery is recharged the power demanded by the bus drops and the EP power increases. Once the bus demand drops the voltage of the SA rises following the IV curve, as seen in Figure 25. This raise in voltage is translated to the discharge supply via the DCX, which translates to an increased power delivery to the HET, as seen in Figure 26.
The effect of the variable SA voltage over the EP can be seen in Figure 26, where the anode voltage and discharge power show a peak of 500V and 1200 W, right out of eclipse when the SA is cold. This peak is translated to an increased thrust and ISP as seen in Figure 27. The effect of the SA increasing its voltage after the MPP is released translates also to the anode voltage, with the effect in the ISP. However, this minor increase in less noticeable in power and thrust.

These results are analogous to the ones in the Separated SA architecture. The power extracted from the two SA are represented in Figure 28. Out of eclipse both SAR modules are locked into the MPP of the correspondent SA. When the battery is fully charged one of the SA, the one only supplying the bus (SA_BUS), comes out MPP. This is apparent in Figure 28 where the power extracted from SA_BUS is smaller than the maximum power available in said SA. The power extracted from the SA_EP goes part to the bus (cyan trace in Figure 28) part to the EP (green trace in Figure 28). It is also apparent in the voltage ober the SA and its V_{mp}, represented in Figure 29. It can be seen how the SA_EP is always at is V_{mp} voltage while the voltage on the SA_BUS increases once the battery is charged and the SAR locks out of the MPP.
Therefore, the variations in voltage to the SA_EP are smaller, since it is sized to power the EP_SA and small extra margin for the bus. This makes its voltage locked to MPP as soon as EP is powered. However, the variation related to the temperature are still present and reflect on the EP voltage, represented in Figure 30, and in the ISP and thrust as represented in Figure 31. As the SA reaches its final temperature the voltage and power are well regulated and unaffected of the changes in the power demanded to the bus. However, there is still the peak power at the exit of eclipse when the SA is cold. The effect of such changes in thrust and ISP must be recognized by EP experts. Also there may be an impact on the orbital dynamics which need to be addressed by mission analysists.
Two tests have been performed to determine which architecture would be better for the application. In the first one the number of strings in parallel have been tailored so the power extracted in each case allows the SC to recharge the battery after each eclipse. Results can be seen in Table 1. The Time recharge column is the time at which the battery is recharged after an eclipse at time 7365 s. It can be seen in the simulation because the SA comes out of MPP. It can be seen how PPU architecture can deliver more power to the battery than the newly proposed ones. The time to recharge is significantly smaller, showing that more power is delivered to the battery. However, the SA has one more string than the Single SA architecture and 2 more than the Separated SA, implying that the SA is bigger and has a bigger mass. The same can be inferred from the other two architecture Times to recharge are longer but the SA are smaller too.

Architecture	Strings SA	Strings EP SA	Time to recharge(s)
Traditional PPU	46		1965
Single SA	45		2025
Separated SA	23	21	2145

Table 1: Architecture comparison

To make a fairer comparison, the power to the EP is regulated to the same power as the one achieved by the PPU and the PPU_DCX architectures and the number of strings is the same in all the cases. In this case the power is regulated by sensing the voltage over the anode and adjusting the discharge current via gas flow control, so the power is constant. Thus a multiplication of the anode voltage and discharge current is needed. The control loop, together with the rest of the system, is shown in Figure 32 for the Single SA architecture.

The results can be seen in the following figures. Figure 33 shows the power extracted from the SA. It does not differ much from the results of the Single SA without the regulated discharge power as seen in Figure 24. However, the input power to the DCX supplying he discharge now it is constant.
The action of the control loop can be seen in Figure 34, where it can be seen how the power of the discharge is constant regardless the voltage across the anode of the thruster. Power is regulated so if voltage increases, as it happens when the battery charges and the SA moves away MPP, the current decreases. This reflects in the thrust, related to the current. As seen in Figure 35 as the voltage rises so does the ISP, but the thrust, which is related to the current decreases.

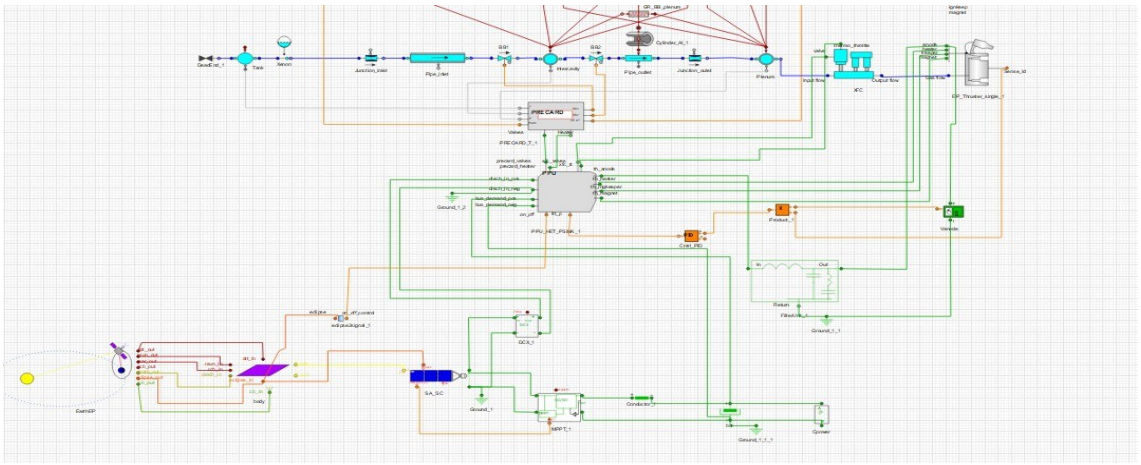

Figure 32: Single SA architecture with constant discharge power

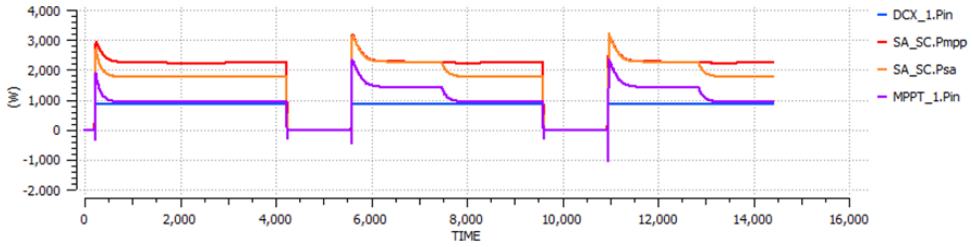

Figure 33: Powers in Single SA architecture with regulated discharge power

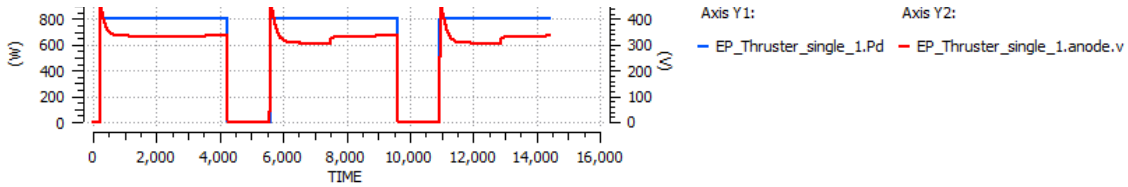

Figure 34: Anode voltage and thruster power in Single SA architecture with regulated power

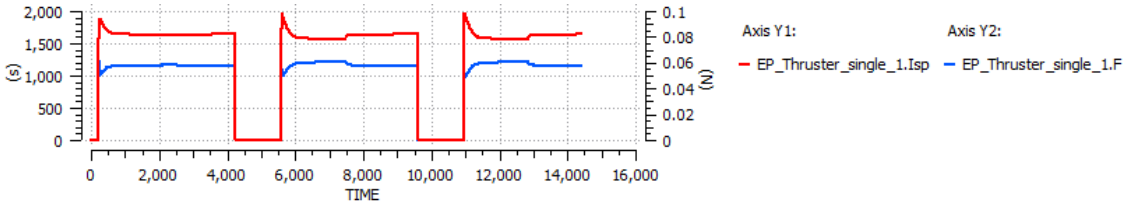

Figure 35: ISP and thrust in Single SA architecture with regulated power

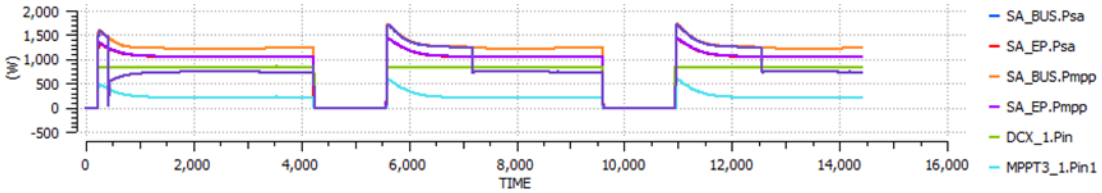

Figure 36: Powers in Separated SA architecture with regulated discharge power

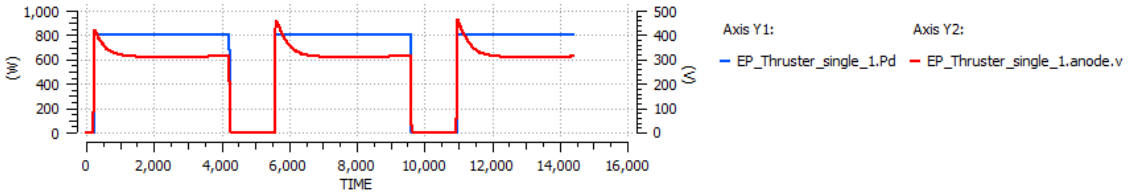

Figure 37: Anode voltage and thrustere power in Separated Sa architecture with regulated power

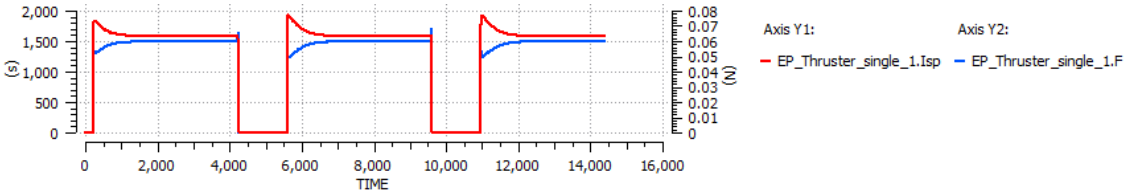

Figure 38: ISP and thrust in Separated SA architecture with regulated power

The results using the Separated SA architecture with the same power regulation control loop are very similar. Powers extracted from the different SAs are represented in Figure 36, where it can be seen how SA_EP is always at its MPP. Thanks to this the voltage to the anode is more regulated, showing only the variations due to SA temperature, as seen in, scaled to the anode voltage through the DCX, in Figure 37. It is also apparent how the EP power remains constant. The effect of the voltage variation then reflects in the ISP and thrust ratio seen in Figure 38.

With this approach it Is guaranteed that all solutions deliver the same power to the EP. SAs have been changed so in all the solutions they have the same number of strings, so the same power installed. Results can be seen in Table 2. The time of the simulation is slightly different, so the eclipse happens at time 5594 s. The time to recharge the battery is significantly lower in the architectures Single SA and Sep SA, showing that they can deliver more power to the battery. Therefore, smaller SAs can fulfil the SC mission. Note that the EP SA is the same in both tests since it was enough to supply the EP. The extra power installed in the Separated SA architecture is devoted to the bus and then to recharge the battery. This flexibility is an advantage of the Separated SA architecture.

Architecture	Strings SA	Strings EP SA	Time to recharge
PPU	46		1956
Single SA	46		1706
Separated SA	25	21	1586

Table 2: Architecture comparison regulating EP power

The option to regulate the power of the discharge via the gas flow was taken here. However other options are possible. For the Separated SA architecture, it could be possible to regulate the input voltage to the DCX, through a control loop that will control the current injected in the bus by the SAR module connected to it. For the Single SA option, it would be possible to regulate the DCX input voltage via the gas flow control. Both options have not been simulated in ECOSIM and are a matter of future works. The necessity to do so to regulate the thrust or the ISP needs to be assessed by Electric Propulsion experts. Other effects on the HET, such as displacement of the thrust vector, have not been evaluated but since the ECOSIM thruster model offers it could be easily done.

VII. Conclusions

The usage of ECOSIM to simulate both the power system using PEPS and the EP system using ESPSS libraries have demonstrated to be very useful. It allows to show the interactions between the electrical power system and electrical propulsion showing interesting information to both designers. Coupled to simple orbital simulations, as the ones used in PEPS, it becomes a great tool to provide power balance analysis. Moreover, it allows to explore different control methods to the HET, whether controlling the power or the thrust or the ISP.

The effects of the variable thrust and ISP due to the lack of regulation of the SA voltage typical from DD architectures is reported in this work. Its impact on mission analysis is outside the scope of this work and would be, together with the effect of this variations on the HET, an interesting multidisciplinary research topic.

To enhance its capabilities some developments could be used in ESPSS libraries. Probably the most relevant ones in this research activity would be the modelling of the HET discharge oscillations and the possibility of a discharge between the anode and the SC structure. Both are very complicated matters involving plasma physics, however even a crude approximation would be very welcome for the integrated use of PEPS and ESPSS.

VIII. Bibliography

[1] J.-P. Boeuf, 'Tutorial: Physics and modeling of Hall thrusters', *J. Appl. Phys.*, vol. 121, no. 1, p. 011101, Jan. 2017, doi: 10.1063/1.4972269.

[2] D. M. Goebel and I. Katz, *Fundamentals of electric propulsion: ion and Hall thrusters*. in JPL space science and technology series, no. 1. Hoboken, N.J: Wiley, 2008.

[3] J. A. Hamley, ‘Direct drive options for electric propulsion systems’, *IEEE Aerosp. Electron. Syst. Mag.*, vol. 11, no. 2, pp. 20–24, Feb. 1996, doi: 10.1109/62.484301.

[4] John Steven Snyder, John R.Brophy, Richard R. Hofer, Dan M. Goebel, § and Ira Katz, ‘Experimental Investigation of a Direct-Drive Hall Thruster and Solar Array System at Power Levels up to 10 kW’,

[5] T. A. Schneider *et al.*, ‘Solar Arrays for Direct-Drive Electric Propulsion: Arcing at High Voltages’, *J. Spacecr. Rockets*, vol. 42, no. 3, pp. 543–549, 2005, doi: 10.2514/1.5636.

[6] I. G. Mikellides, G. A. Jongeward, T. Schneider, T. Peterson, T. W. Kerslake, and D. Snyder, ‘Solar Arrays for Direct-Drive Electric Propulsion: Electron Collection at High Voltages’, *J. Spacecr. Rockets*, vol. 42, no. 3, pp. 550–558, 2005, doi: 10.2514/1.5609.

[7] Miaja, Andreas Franke, Christian Brandt, Denis Estublier, and Manuel Arias, ‘Comparative of different Direct Drive architectures’, presented at the European Space Power Conference, Elche, Spain, Oct. 2023.

[8] A. K. Podder, N. K. Roy, and H. R. Pota, ‘MPPT methods for solar PV systems: a critical review based on tracking nature’, *IET Renew. Power Gener.*, vol. 13, no. 10, pp. 1615–1632, 2019, doi: 10.1049/iet-rpg.2018.5946.

[9] A. Fernandez, C. Baur, and F. Gomez-Carpintero, ‘Solar Array Hysteresis and its Interaction with the MPPT System’, presented at the European Space Power Conference, Noordwijk, Netherlands, 2014.

[10] ‘GOCE System System Critical Design Review’. May 2015.

[11] A. Caon, M. Doerre, J. E. Haines, and S. Landstroem, ‘The GOCE electrical power system’, in *IECEC ’02. 2002 37th Intersociety Energy Conversion Engineering Conference, 2002.*, Jul. 2002, pp. 87–92. doi: 10.1109/IECEC.2002.1391984.